

Intermolecular Potentials for Ammonia-Aqueous Mixture

J. Rzepkowska

Industrial Chemistry Research Institute, Rydygiera 8, 01-793 Warsaw, Poland

N. Uras

*Fritz Haber Institut for Molecular Dynamics, Hebrew University, Jerusalem, 91904, Israel, and
Department of Chemistry, Oklahoma State University, Stillwater, Oklahoma 74078*

J. Sadlej*

Department of Chemistry, University of Warsaw, Pasteura 1, 02-093 Warsaw, Poland

V. Buch

Fritz Haber Institut for Molecular Dynamics, Hebrew University, Jerusalem, 91904, Israel

Received: October 12, 2001; In Final Form: December 18, 2001

The results of the second-order Møller–Plesset perturbation theory calculations with the aug-cc-pvTZ basis set for the $\text{NH}_3\cdots\text{H}_2\text{O}$ complex have been used to parametrize a set of atom–atom potentials. A simple nonpolarized and polarized ammonia–water potential is proposed. The quality of these potentials has been tested by performing the rigid body Diffuse Monte Carlo calculations of the energetics, rotational and quadrupole coupling constants for dimer $\text{H}_2\text{O}\cdots\text{NH}_3$. The present potentials are the first ones predicting the structures of the trimers $(\text{H}_2\text{O})_2\cdots\text{NH}_3$ and $(\text{NH}_3)_2\cdots\text{H}_2\text{O}$ confirmed by ab initio calculations. These potentials were successfully used in Monte Carlo simulations of the interaction of ammonia with an ice particle (N. Uras, V.; Buch, J. P.; Devlin, J. *Phys. Chem. B* 2000, 104, 9203).

I. Introduction

Over the past years, a number of papers have appeared in which the properties of ammonia in the liquid and solid phases have been calculated on the basis of atom–atom potential functions (see, for instance refs 1–5). Also, the effective pair-potential models, parametrized for the properties of the pure liquids have been used in molecular dynamics simulations of liquid water.² Interest in these works was mainly focused on the structure of one-component systems. However, aqueous mixtures, such as those containing ammonia have found several scientific and industrial importance. Water and ammonia are known to be two of the most important molecules in chemical evolution studies,^{6,7} and in interstellar chemistry.^{8–10} As a major trace gas of the atmosphere, the transport of ammonia across the air–water interface is very important in atmospheric chemistry, see ref 11. Some of the experimental work mentioned above has been accompanied by simple theoretical investigations aimed at the proper interpretation of the data and better understanding of the processes involved. Necessary for all research of this type is the knowledge of the interaction between water and ammonia molecules.

Many studies revealed that the clustering between water and ammonia is extensive and predominant over formation of pure water or pure ammonia clusters.^{12,13} This is consistent with the theoretical predictions showing that the $\text{NH}_3\cdots\text{H}_2\text{O}$ mixed clusters have larger hydrogen-bond energy than those of the corresponding homonuclear clusters.^{14–17}

Recently, the $\text{NH}_3\cdots\text{H}_2\text{O}$ complex was examined by microwave and tunable far-infrared laser spectroscopy.^{18,19} The spectroscopic constants were published, obtained from micro-

wave and radio frequency spectra, observed by molecular beam electric resonance spectroscopy.²⁰ The detailed microwave study by Stockman et al.¹⁸ provides the equilibrium structure of the complex. Second group of papers for gaseous complex is devoted to the matrix isolation studies of $\text{NH}_3\cdots\text{H}_2\text{O}$ in the Ar, Ne, and Kr matrixes. Nelander et al.^{21,22} and Yeo and Ford²³ registered vibrational frequencies of the ammonia and water intramolecular modes and several intermolecular modes of the complex. Because of the atmospheric importance, the study the adsorption of ammonia on the ice nanocrystals was investigated in ref 24 as an example of the formation of “active” adsorbates, which are attached to the ice surface and modify the hydrogen bonding network.^{25,26}

The aim of the experimental studies of weakly bound complexes is to obtain both the structures and the potential functions. Indeed, a successful determination of the potential energy surfaces for van der Waals and hydrogen-bonded complexes has so far been possible only for atom-molecule complexes. See, for instance, refs 27, 28. Only recently, powerful dynamical techniques have been developed for refinement of the potential surfaces of systems as large as the water dimer.²⁹

A complementary approach to obtain structural and potential function information for weakly bound complexes are the ab initio calculations. Although the accuracy of the ab initio calculations is still below the state-of-the-art accuracy of the spectroscopic data, the calculations provide information on the shape of the potential energy surfaces without any initial assumptions.

Previous ab initio potential energy surfaces for the most stable conformers of $\text{NH}_3\cdots\text{H}_2\text{O}$ were reported in a few papers.^{30–35}

Recently, optimal structures, interaction energies, and harmonic vibrational frequencies of the $\text{NH}_3 \cdots \text{H}_2\text{O}$ complex have been determined from the second-order Møller–Plesset perturbation theory calculations with the aug-cc-pVTZ basis set.³⁶ The nature of the intermolecular interactions in the complex was investigated by symmetry-adapted perturbation theory (SAPT). As revealed by the SAPT analysis, the main binding contributions are the electrostatic and induction components.

Most of the simulations to date used “effective” pair potentials: simple empirically parametrized model potential. In contrast to other systems for which numerous intermolecular potentials was proposed in the literature, there was only one Monte Carlo simulation of aqueous ammonia solution based on minimal basis set calculations for the complex.³⁷ However, a small basis set used and the neglect of the BSSE correction put in question the reliability of this potential.

This work belongs to a series of our theoretical investigations of H_2O complexes with small molecules using the combination of ab initio calculations and Diffusion Monte Carlo (DMC) evaluations.^{39–41} Understanding of weak interactions between H_2O and other molecules is needed, for example in study of molecular solvation in water and ice and in investigations of gas adsorption on icy surface. This paper was stimulated by recent experimental study of ice nanocrystals with ammonia.²⁴ It presents a new water–ammonia pair potential obtained by means of ab initio calculations. Potentials describe here was used in Monte Carlo simulations to calculate the structure of the ice-adsorbate system as a function of coverage.³⁸ The goal of this paper is thus 3-fold: (i) to compute the potential energy surface of the $\text{NH}_3 \cdots \text{H}_2\text{O}$ complex and to study the effect of the rotation of the water and ammonia molecules on the shape of this surface; (ii) to construct the nonpolarizable and polarizable potential of this system which yields a fair description of certain properties of the condensed phases of aqueous mixture of ammonia; (iii) to calculate the dimer rotational and quadrupole coupling constants averaged over the zero-point motion by Diffusion Monte Carlo method (DMC) and to utilize the potential for the determination of the possible structure of the mixed trimers assuming pairwise interaction between molecules in the clusters. This paper is organized as follows. In section II, we briefly describe the ab initio and DMC calculations carried out in this work. In section III, we present different methodologies for construction of the potentials. Section IV discusses the shape of the potential energy surface obtained for the dimer from ab initio calculations and the results of DMC calculations. Finally, section V concludes our paper.

II. Methods of Calculations

A. Supermolecular Calculations. The supermolecular calculations have been done with the Gaussian 94⁴² program in two stages. First, full geometry optimizations have been carried out using the MP2 method for the isolated subunits and for the entire complex. The vibrational frequencies have been computed within the harmonic approximation at the MP2 level. All calculations were performed on frozen core approximation. The interaction energy of the complex, $E_{\text{int}}^{\text{MP}n}$, $n = 2, 4$ has been obtained by subtraction of the energies of complex and of the monomers. In the calculations of the interaction energies, we employed the full basis of the dimer, i.e., we corrected the computed interaction energies for the basis-set superposition error using the prescription of Boys and Bernardi.⁴³ This is a commonly accepted procedure to obtain reliable interaction energies,^{44,45} despite some controversial arguments reported in the literature.⁴⁶ Dissociation energies $D_0^{\text{MP}n}$ were obtained from

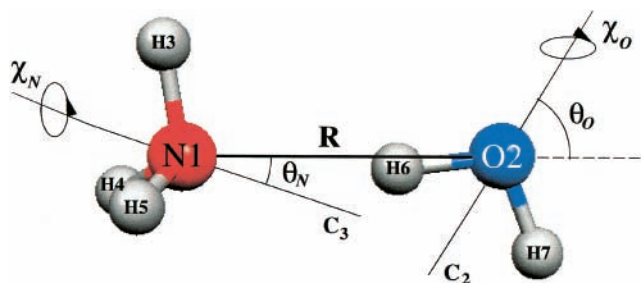


Figure 1. Definition of cluster coordinates.

the interaction energies by adding the correction for the zero-point vibrational motion. In our work, the zero-point correction was calculated at the MP2 level. Dissociation energies is not corrected for deformation error. In these complexes, the deformation error is quite small, as was shown in ref 36. We made no attempt to optimize the complexes including the CP correction, although methods for doing this have been recently suggested.⁴⁷ This means that no account has been taken of BSSE in the optimized geometries and harmonic frequencies.

In the second stage, the points on the potential energy surface (PES) have been calculated using the second-order Møller–Plesset perturbation theory (MP2). In the PES calculations, the monomer geometries were kept constant: for water $r(\text{OH}) = 0.9572 \text{ \AA}$, $\text{HOH} = 105.52^\circ$; for ammonia $r(\text{NH}) = 1.01242 \text{ \AA}$, $\text{HNH} = 106.67^\circ$. The coordinate system is shown in Figure 1. The interaction energy $E_{\text{int}}^{\text{MP}2}$ was calculated as a function of \mathbf{R} , where \mathbf{R} is a radius vector connecting the nitrogen and oxygen atoms. For each orientation of the intermolecular axes \mathbf{R} , the potential was calculated as a function of six angles: θ_N and θ_O between the symmetry axis C_3 or C_2 and the intermolecular axis; two angles χ_N and χ_O , which describe the rotation of ammonia and water molecules about their symmetry axes and two angles: ϕ_O and ϕ_N which describe the motion of the symmetry axes C_2 and C_3 out of $\text{O}2\text{N}1\text{H}3$ plane (see Figure 1).

We decided to use the aug-cc-pvTZ atomic basis.⁴⁸ As shown by Xantheas et al.^{49–51} this basis set accurately reproduces the geometries, frequencies and electric properties of isolated molecules and their complexes and was used by us in many papers.^{36,52,53}

B. DMC Calculations. Weakly bonded clusters tend to be floppy and, thus, are better represented by a distribution of configurations corresponding to the zero-point motion, than by a single minimum energy configuration. Diffusion Monte Carlo (DMC) is a convenient numerical method to study clusters in their ground vibrational states. Here, DMC is employed to calculate the dimer rotational and quadrupole coupling constants averaged over the zero-point motion, using fitted potentials described above. The resulting values are compared to experiment. In addition, mixed water–ammonia trimers are investigated.

Rigid body DMC (RBDMC) is a numerical method to solve the time independent Schrödinger equation by a random walk of a cloud of replicas of a quantum system. Here, we provide only a brief summary of the method. The basic DMC algorithm is described in refs 54, 55 the rigid body version is given in ref 56. Applications to other cluster systems can be found, e.g., in refs. 40, 41, 56.

The method is based on the substitution of $\tau = it$ in the Schrödinger equation, converting of it to the diffusion equation. The formal solution is

$$\sum_n C_n j_n \cdot \exp(-tE_n/h) \quad (1)$$

where j_n denotes an eigenstate of the Hamiltonian, E_n is the corresponding energy and C_n is an arbitrary expansion coefficient. In the long time limit, the density of the cloud of replicas mimics the ground state. The random-walk method to find the ground state of the system is a simulation of a process containing random movements (random translation and rotation of molecules in the replicas), and multiplication/disappearance of replicas of low/high potential energy, respectively.^{40,54,56} The calculation employed 2000 replicas, and a time step of 30 atomic units. Expectation values of quadrupole coupling and rotational constants, and of other geometric properties, averaged over the instantaneous configurations generated by the simulation, were calculated as in ref 40, using the descendent weighting method.⁵⁵

III. Intermolecular Potentials

In this study, we obtained two intermolecular potential functions for the ammonia–water system: nonpolarizable and polarizable potential energy surfaces (PES). The PES were constructed as analytical fits to 850 ab initio points. Then DMC calculations were carried out for the ground vibrational state (gvs), and for rotational and quadrupole coupling constants averaged over gvs; the results were compared to the experimental data. In all these calculations, the ammonia and water geometric parameters were assumed rigid and equal to the parameters used in the ab initio mapping.

A. Nonpolarizable Potential. For describing the energy surface analytically, the ammonia–water intermolecular potential is represented as a sum of electrostatic interactions between charge sites on each molecule and a single Lennard–Jones (12–6) term between nitrogen and oxygen atoms

$$V_{ij} = 4\epsilon((\sigma/r_{ON})^{12} - (\sigma/r_{ON})^6) + \sum_{ij} (q_i q_j / r_{ij}) \quad (2)$$

where r_{ij} denotes intermolecular distance between point charges q_i and q_j . A similar form of potential was employed successfully in the past for the $\text{H}_2\text{O}\dots\text{H}_2\text{O}$ (e.g., 2) and $\text{NH}_3\dots\text{NH}_3$ ³ interactions.

The point charges and their positions for NH_3 and H_2O were adopted from the work of Tanabe and Rode.³⁷ The fitted nonpolarizable potential included three point charges on H_2O and four point charges on NH_3 . The positive charges were placed at the H-atoms, $q = 0.62e$ for H_2O , and $q = 0.462e$ for NH_3 . The negative charges were placed on the water C_2 axis and on the ammonia C_3 axis, 0.2677 and 0.156 Å from O and N, toward the H-atoms, respectively. For Lennard–Jones terms, we used $\text{NH}_3\text{--}\text{NH}_3$ and $\text{H}_2\text{O}\text{--}\text{H}_2\text{O}$ dimer terms and applied Lorentz–Berthelot mixing rules.⁵⁷ The Lennard–Jones parameters were further adjusted to fit the ab initio points with final values of $\epsilon = 0.2076$ kcal/mol and $\sigma = 3.27$ Å. For the entire PES region, the standard deviation between the fit and ab initio points was 1071 cm^{-1} and, in the negative PES region, 114 cm^{-1} .

B. Polarizable Potential. The polarizable potential was composed of pairwise-additive energies (Coulomb and Lennard–Jones terms) and the energy associated with the induced dipoles. The pair-additive part is of the same functional form as the nonpolarizable potential; its parameters are also the same except for Lennard–Jones $\sigma = 3.285$ Å. A single dipole polarizability center was placed on the water C_2 axis and on the ammonia C_3 axis, 0.48 Å from O and N, respectively, toward the H-atoms (as in the water potential MKW, described in ref 58). Experimental polarizabilities were used for water ($\alpha = 1.429$ Å³) and ammonia ($\alpha = 2.226$ Å³). Discussion of energy terms associated with induced dipoles can be found in Ref 59.

Briefly, for a many body system consisting of point charges and point dipoles, the dipole polarization energy can be given by the following equation⁶⁰

$$V = -(1/2) \sum_{i=1}^N p_i \cdot E_i^0 \quad (3)$$

where p_i is the induced dipole moment at molecule i

$$p_i = \alpha_i E_i = a_i (E_i^0 + \sum_{j=1, j \neq i}^N T_{ij} p_j) \quad (4)$$

α_i is the polarizability of molecule i and N is the number of molecules in the system. E_i^0 is the electrostatic field from the charges

$$E_i^0 = f_s \left(\sum_{j=1, j \neq i}^N q_j r_{ij} / r_{ij}^3 \right) \quad (5)$$

where q_j is the charge at site j , r_{ij} is the vector from charge site j to polarizability center i . The dipole tensor, T_{ij} is given by

$$T_{ij} = ((3r_{ij} r_{ij} / r_{ij}^2) - 1) / r_{ij}^3 \quad (6)$$

where r_{ij} denotes the distance between two polarizability centers. To avoid numerical instabilities at short distances, a “shielding factor” f_s is employed for electrical fields of point charges of H-atoms, calculated at the polarizability centers. (For the negative charges, $f_s = 1$). The form of the shielding factor was adopted from ref 59

$$f_s = 1 - \exp(-r_s^2 / r_{ij}^2) \quad (7)$$

where $r_s = 1.75$ Å, and r_{ij} denotes a distance between an H-atom, and a polarizability center.

IV. Results and Discussion

A. Shape of the Potential Energy Surface. The main features of the interaction potential between water and ammonia molecules are determined by the symmetry of the complex. Ab initio calculations at the MP2/aug-cc-pvTZ level predicted for the dimer a global minimum corresponding to the trans conformer (Figure 2a). The cis conformer (Figure 2b) is a saddle point (one imaginary frequency).³⁶ The optimized geometries, which are the global minima on PES at the MP2/aug-cc-pvTZ level for the two trimers $(\text{H}_2\text{O})_2\dots\text{NH}_3$ and $(\text{NH}_3)_2\dots\text{H}_2\text{O}$ are illustrated in Figure 2c and 2d too.

Table 1 presents the energetics of the complexes: the dimer and two trimers. The ab initio calculation for the trimer $(\text{H}_2\text{O})_2\dots\text{NH}_3$ has been reported in ref 11, whereas the trimer $(\text{NH}_3)_2\dots\text{H}_2\text{O}$ has been investigated, to our knowledge, neither experimentally nor theoretically. The fact that the cis structure of $\text{NH}_3\dots\text{H}_2\text{O}$ differs only marginally from the trans one supports the conclusion of the earlier theoretical and experimental findings that the ammonia molecule in the complex is almost free to rotate about its C_3 axis. Inclusion of the correlation effects at the MP2 level is important and increases the interaction energy from -4.468 kcal/mol to -6.323 kcal/mol for trans form, i.e., by about 40%. The MP4 calculations for the dimer change slightly this number and give nearly identical results. For the structures of the dimer considered in Table 1 the convergence of the Møller–Plesset expansion for the interaction energy appears to be good, the MP2 approximation providing over 97% of the MP4 result for both, the trans and cis geometries of

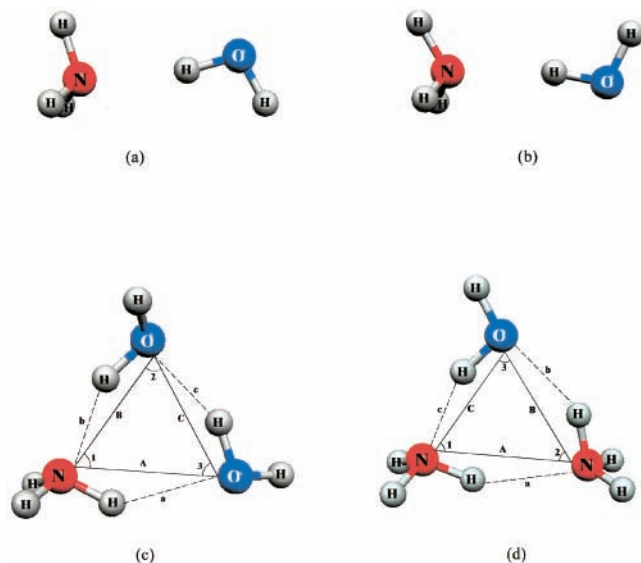


Figure 2. Geometries (MP2/aug-cc-pvTZ) of the $\text{H}_3\text{N}\cdots\text{HOH}$ complex corresponding to the (a) trans, (b) cis conformers of $\text{H}_2\text{O}\cdots\text{NH}_3$ and global minima of the trimers, and (c) $(\text{H}_2\text{O})_2\cdots\text{NH}_3$ and (d) $(\text{NH}_3)_2\cdots\text{H}_2\text{O}$.

TABLE 1: Interaction Energies, and Dissociation Energies (in kcal/mol) for the trans, cis Conformers of the $\text{NH}_3\cdots\text{H}_2\text{O}$ Complex and for the Trimers $(\text{H}_2\text{O})_2\cdots\text{NH}_3$, $(\text{NH}_3)_2\cdots\text{H}_2\text{O}$ Calculated at the MP2/Aug-cc-pvTZ Level. (ZPE correction calculated at the MP2 level)

	$\text{H}_2\text{O}\cdots\text{NH}_3$ trans	$\text{H}_2\text{O}\cdots\text{NH}_3$ cis	$(\text{H}_2\text{O})_2\cdots\text{NH}_3$	$(\text{NH}_3)_2\cdots\text{H}_2\text{O}$
$E_{\text{int}}^{\text{HF}}$	-4.468	-4.472	-10.416	-8.287
$E_{\text{int}}^{\text{MP2}}$	-6.365	-6.361	-15.520	-13.577
$E_{\text{int}}^{\text{MP4}}$	-6.323	-6.320	-15.402	-13.454
D_0^{HF}	1.787		5.406	3.789
D_0^{MP2}	3.990		10.510	9.079
D_0^{MP4}	3.969		10.393	8.956

$\text{NH}_3\cdots\text{H}_2\text{O}$, respectively.³⁶ As one can see from the Table 1, there is a significantly greater binding energy of ammonia to two hydrogen-bonded water molecules in the trimer $(\text{H}_2\text{O})_2\cdots\text{NH}_3$ than there is to a single water molecule. This energy arises from the formation of a second hydrogen bond with ammonia molecule acting as a donor of electron and the second water molecule acting as the acceptor of H-bond. For the trimer $(\text{NH}_3)_2\cdots\text{H}_2\text{O}$, one can notice also the greater binding energy of water to two hydrogen-bonded ammonia molecules than there is to a single ammonia molecules in the complex $\text{H}_2\text{O}\cdots\text{NH}_3$. A second ammonia molecule forms the H-bond with water molecule as a donor of H-bond and with the second ammonia molecule as an acceptor of H-bond. The experimental dissociation energy of this dimer and trimers is not known. Extensive calculations of the binding energies of van der Waals complexes indicate that our value calculated in the aug-cc-pvTZ basis set is underestimated, mainly due to an underestimation of the dispersion component of the interaction energy, by about 10–15%.⁶¹

B. Tunneling Motion of the Molecules in the Complex.

We are turning now to the internal motion of the molecules in the dimer $\text{H}_2\text{O}\cdots\text{NH}_3$. We investigated the energetics of the NH_3 rotation about the C_3 axis of ammonia (described by the angle χ_N) and H_2O rotation about the C_2 axis of water (described by the angle χ_O). These results are shown in Figures 3 and 4. The trans structure corresponds to $\chi_N = 0^\circ$, the cis one to $\chi_N = 60^\circ$. The MP2 energy difference trans-cis is equal to 0.41 cm^{-1} only. Taking into account the minimum energy path connecting the

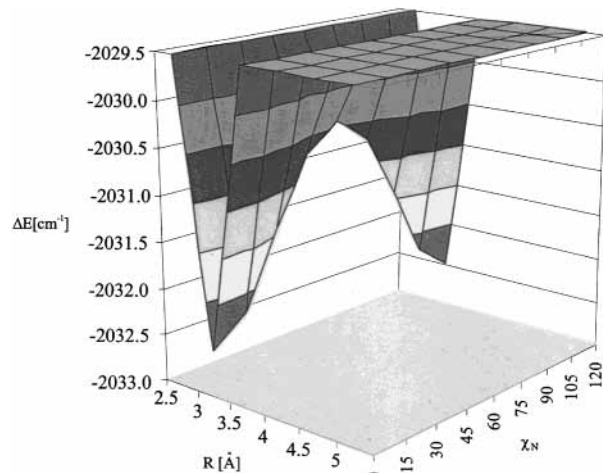


Figure 3. Interaction energy for the rotation of the ammonia molecule at the MP2/aug-cc-pvTZ level as a function of R and χ_N for the configuration $\theta_O = 48^\circ$, $\theta_N = \chi_O = \phi_O = \phi_N = 0^\circ$.

cis and trans forms we found a barrier of 2.2 cm^{-1} . The experimental estimate of this barrier height is $10.5 \pm 5.0 \text{ cm}^{-1}$.¹⁸ Experimentally, the height of the barrier (V_3) was obtained by fitting the parameter V_3 in the potential term of the nuclear motion Hamiltonian to the observed microwave spectra.¹⁸ The agreement between theory and experiment is not perfect. However, this barrier is very difficult to determine, both theoretically and experimentally, due to the extreme flatness of the potential energy surface in this region.

The H_2O tunneling motion is strongly coupled to the ammonia internal rotation (see Figure 4). Contrary to the nearly free rotation of ammonia about its C_3 axis, water rotation about its symmetry axis have a barrier at $\chi_O = 90^\circ$. This point on PES is the saddle point, which corresponds to the bifurcated structure of the complex.³⁶ Taking into account the minimum energy path, which involves the optimization of all the geometrical parameters for all the points except for the $\text{N1}\cdots\text{O2H7}$ angle, we found the barrier of 1267 cm^{-1} . Experimentally, the barrier height was estimated to 840 cm^{-1} ¹⁸ if only the motion of the water subunit was considered in the tunneling process. The theoretical value of the barrier is considerably higher than the experimental one.¹⁸ It is possible that further lowering of the rotation barrier can be obtained by introducing more polarization functions to the basis set.

C. Application of the Potential Function to the Dimers and Trimers. DMC Results. The final PES calculated from the nonpolarizable potential (dashed lines) is shown in Figure 5 for different configurations of the ammonia–water dimer. For the entire PES region, the standard deviation between the fit and ab initio points was 1071 cm^{-1} and, in the negative PES region, 114 cm^{-1} . The final polarizable PES for the different configurations is shown in Figure 5 using solid lines. Over the entire PES region, the standard deviation between the fit and ab initio points was 1111 cm^{-1} and, in the negative PES region, the standard deviation between the fit and ab initio points was 90 cm^{-1} .

The results of the rotational and quadrupole coupling constants averaged over the zero-point motion for the dimer are given in Table 2. The numerical accuracy of the rotational B and C constants is several tens MHz.^{40,41} The A constant is much more difficult to calculate accurately, using the simple version of rotational constant evaluation employed in this DMC study, and the numerical accuracy does not exceed several percent.⁴¹ The calculated and experimental values agree within the accuracy of the DMC method.

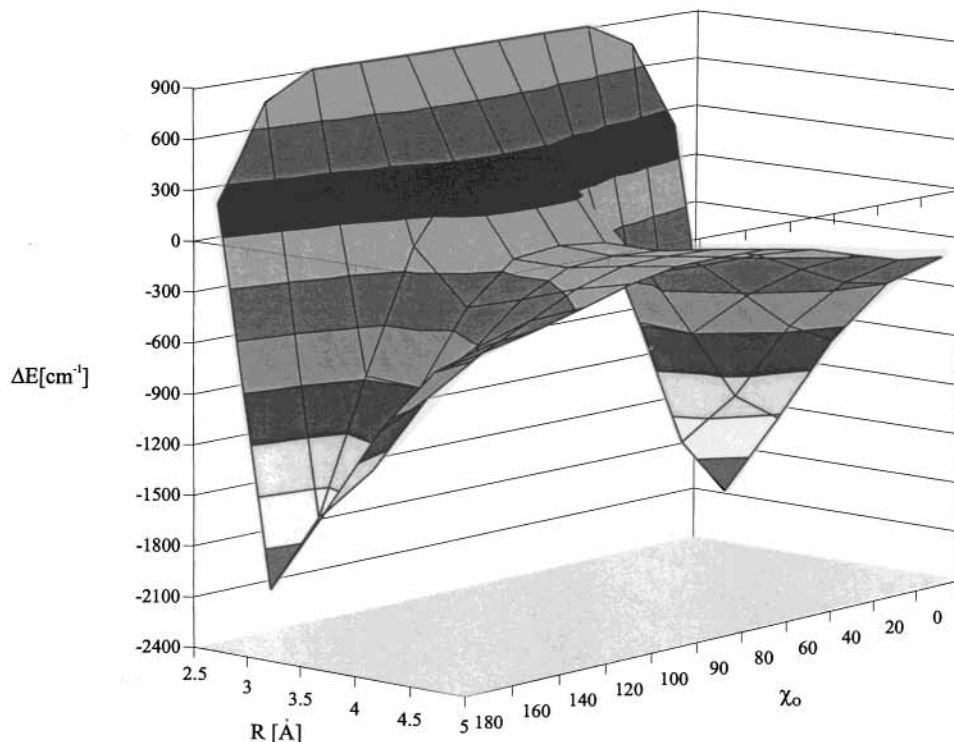


Figure 4. Interaction energy for the rotation of the water molecule at the MP2/aug-cc-pvTZ level as a function of R and χ_0 for the configuration $\theta_O = 48^\circ$, $\theta_N = \chi_N = \phi_O = \phi_N = 0^\circ$.

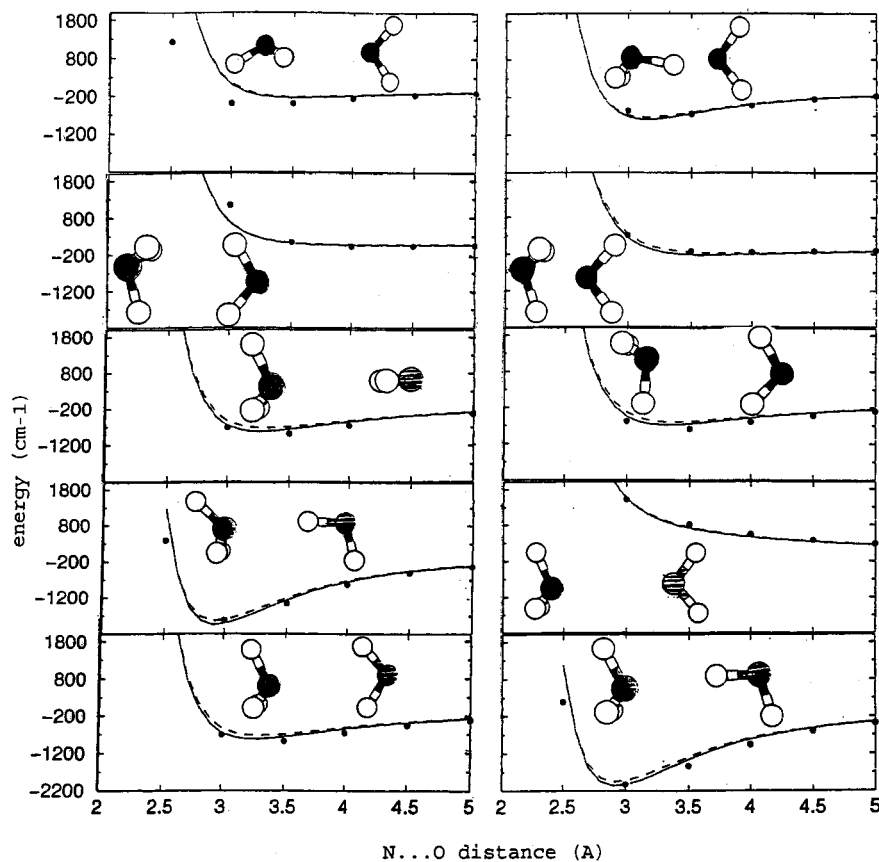


Figure 5. PES calculated from the nonpolarized (dashed lines) and polarized (solid lines) potential for different configurations of the ammonia-water dimer.

A potential surface for the dimer can be utilized to determine the possible structures of larger clusters, assuming pairwise interactions between molecules in the cluster. Both $(\text{NH}_3)_2 \dots \text{H}_2\text{O}$ and $(\text{H}_2\text{O})_2 \dots \text{NH}_3$ complexes were investigated. Two sets of

DMC simulations were run, with the nonpolarizable and polarizable potentials. For $\text{H}_2\text{O} \dots \text{H}_2\text{O}$, TIP4P potential was used in the nonpolarizable case,² and the MKW potential of ref 58 in the polarizable one. The nonpolarizable and polarizable

TABLE 2: Rotational and Quadrupole Constants (in MHz) for the trans Conformer of the NH₃...H₂O and ND₃...D₂O Complex

variable	non-polarizable	polarizable	exp 18
NH ₃ ...H ₂ O			
A(MHz)	152 666	152 184	147 714
B(MHz)	6149	6196	6169
C(MHz)	6094	6140	6111
quadrupole const.	-3.040	-3.156	-3.126
ND ₃ ...D ₂ O			
A(MHz)	77394	76871	
B(MHz)	5258	5301	5220
C(MHz)	5183	5225	5142
quadrupole const.	-3.208	-3.326	-3.344

TABLE 3: Comparison of the Geometrical Parameters (distances in Å Angles in Degrees) of the (H₂O)₂...NH₃ and (NH₃)₂...H₂O Trimers Calculated by ab Initio and DMC Methods (all symbols explained at Figure 2c,d)

	(H ₂ O) ₂ ...NH ₃			(NH ₃) ₂ ...H ₂ O		
	ab initio	non-polar	polar	ab initio	non-polar	polar
angles						
1	57.22	57.48	56.68	61.77	60.94	61.05
2	65.27	68.00	67.27	54.50	53.40	54.34
3	57.50	54.61	56.17	63.72	65.79	64.71
heavy atom distance						
A	3.0404	3.20	3.18	3.1293	3.33	3.25
B	2.8082	2.91	2.92	3.0749	3.19	2.92
C	2.7975	2.81	2.84	2.8411	2.93	3.14
heavy atom...H distance						
a	2.2064	2.39	2.30	2.2021	2.43	2.37
b	1.8733	1.99	2.03	2.1625	2.30	2.23
c	1.8779	1.91	2.05	1.8987	2.00	1.99

TABLE 4: Rotational Constants (MHz) Calculated for the (H₂O)₂...NH₃ and (NH₃)₂...H₂O Trimers

rotational const	(H ₂ O) ₂ ...NH ₃			(NH ₃) ₂ ...H ₂ O		
	ab initio	non-polar	polar	ab initio	non-polar	polar
A(MHz)	7176	7136	6864	6609	6379	6397
B(MHz)	5782	5239	5169	5329	4717	4924
C(MHz)	3286	3077	3003	3044	2789	2865

potentials for the NH₃...NH₃ of refs 3 and 62 were used, respectively. The energy of (H₂O)₂...NH₃ at the ab initio minimum geometry is -14.65 kcal/mol for the nonpolarizable potential, and -14.53 kcal/mol for the polarizable one, as compared to the -15.40 kcal/mol ab initio value at the MP4/aug-cc-pvTZ level. The energy of (NH₃)₂...H₂O at the ab initio minimum geometry is -11.42 kcal/mol for the nonpolarizable potential, and -12.64 kcal/mol for the polarizable potential, as compared to the -13.45 ab initio value at the MP4/aug-cc-pvTZ level. The trimers in their ground vibrational states (calculated by DMC) maintain the cyclic structure found by ab initio calculations. Geometric properties and rotational constants of the clusters are given in Table 3 and Table 4; the definitions of the different angles and distances are given in Figs 2c,d. The DMC expectation values of the different properties are compared to the ab initio values obtained at the potential minimum in the present study. The agreement of the predicted trimer geometries with ab initio values is quite good.

V. Conclusions

In the present study, we investigated the structural, energetic and spectroscopic properties of the dimer H₃N...H₂O and the mixed trimers (H₂O)₂...NH₃, (NH₃)₂...H₂O by means of supermolecular ab initio and DMC calculations. The calculated results may be summarized as follows:

(i) The equilibrium geometry calculated for the dimer at MP2/aug-cc-pvTZ levels agrees well with the experimental measurements. The trans structure with a nonlinear equilibrium hydrogen bond is a global minimum. The *D*₀ dissociation energy is computed to be -3.969 (MP4) kcal/mol, ca. 30% of which arises from correlation effects.

(ii) A new PES was constructed for the H₂O...NH₃ complex, by fitting ab initio points to an analytic function, followed by the calculations of rotational and quadrupole coupling constants for the different isotopic species. The later quantities were calculated by DMC averaging over the zero-point motion. The agreement with experiment is very good.

(iii) The present potential is the first ab initio potential predicting the proper symmetry of the trimer structures assuming pairwise interactions between molecules in the clusters. Geometries and equilibrium rotational constants for the trimers derived from the fits are satisfactorily similar to the ones predicted by ab initio results. Our results can be utilized by spectroscopists to determine the possible experimental structures of the trimers.

Acknowledgment. We thank Prof. J. P. Devlin for helpful and enlightening discussions on the ammonia-water cluster spectroscopy. This work was supported by the KBN Grant No. 7 T09A 111 21. JS would like to thank the Interdisciplinary Center for Computational Modeling, University of Warsaw, for providing the computer time.

References and Notes

- (1) Kincald, R. H.; Scheraga, H. A. *J. Phys. Chem.* **1982**, *86*, 833.
- (2) Jorgensen, W. L.; Chandrasekhar, J.; Madura, J. D.; Impey, R. W.; Klein, M. L. *J. Chem. Phys.* **1983**, *79*, 926.
- (3) Impey, R. W.; Klein, M. L. *Chem. Phys. Lett.* **1984**, *104*, 579.
- (4) Gao, J.; Xia, X.; George, T. F. *J. Phys. Chem.* **1993**, *97*, 2471.
- (5) Diraison, M.; Martyna, G. J.; Tuckerman, M. E. *J. Chem. Phys.* **1999**, *111*, 1096.
- (6) Leummon, R. M. *Chem. Rev.* **1970**, *70*, 95.
- (7) Ailenhoff, W. J.; Strumpff, P.; Walmsley, M. *Astron. Astrophys.* **1983**, *125*, L19.
- (8) Jackson, W. M. *J. Photochem.* **1976**, *5*, 107.
- (9) Finlayson-Pitts, B. J.; Pitts, B. J., Jr. *Atmospheric Chemistry*, Wiley: New York, 1986.
- (10) Cavazzoni, C.; Chiarotti, L.; Scandolo, S.; Tosatti, E.; Bernasconi, M.; Parinello, M. *Science* **1999**, *282*, 44.
- (11) Donaldson, D. J. *J. Phys. Chem., A* **1999**, *103*, 62.
- (12) Shinohara, H.; Nishi, N.; Washida, N. *Chem. Phys. Lett.* **1984**, *106*, 302.
- (13) Shinohara, H.; Nagashima, U.; Tanaka, H.; Nishi, N. *J. Chem. Phys.* **1985**, *83*, 4183.
- (14) Topp, W. C.; Allen, L. C. *J. Am. Chem. Soc.* **1974**, *96*, 5291.
- (15) Kollman, P.; McKelvey, J.; Johansson, A.; Rothenberg, S. *J. Am. Chem. Soc.* **1974**, *97*, 955.
- (16) Allen, L. C. *J. Am. Chem. Soc.* **1971**, *93*, 4991.
- (17) Sokalski, W. A.; Hariharan, P. C.; Kaufman, J. J. *J. Phys. Chem.* **1983**, *87*, 2803.
- (18) Stockman, P. A.; Bumgarner, R. E.; Suzuki, S.; Blake, G. A. *J. Chem. Phys.* **1992**, *96*, 2496.
- (19) Fraser, G. T.; Suenram, R. D. *J. Chem. Phys.* **1992**, *96*, 7287.
- (20) Herbine, P. T.; Dyke, R. J. *J. Chem. Phys.* **1985**, *83*, 3768.
- (21) Nelander, B.; Nord, L. *J. Phys. Chem.* **1982**, *86*, 4375.
- (22) Engdahl, A.; Nelander, B. *J. Chem. Phys.* **1989**, *91*, 6604.
- (23) Yeo, G. A.; Ford, T. A. *Spectrochim. Acta A* **1991**, *47*, 485.
- (24) Delzeit, L.; Powell, K.; Uras, N.; Devlin, J. P. *J. Phys. Chem.* **1997**, *101*, 2327.
- (25) Delzeit, L.; Devlin, J. P.; Buch, V. *J. Chem. Phys.* **1997**, *107*, 3726.
- (26) Devlin, J. P.; Uras, N.; Rahman, J. M.; Buch, V. *Isr. J. Chem.* **1999**, *39*, 261.
- (27) Hudson, J. M. *Annu. Rev. Phys.* **1990**, *41*, 123.
- (28) Cohen, R. C.; Saykally, R. J. *J. Phys. Chem.* **1992**, *96*, 1024.
- (29) Leforestier, C.; Braly, L. B.; Liu, K.; Elrod, M. J.; Saykally, R. J. *J. Chem. Phys.* **1997**, *106*, 8527.
- (30) del Bene, J. E. *J. Am. Chem. Soc.* **1973**, *95*, 5460; del Bene, J. E. *J. Phys. Chem.* **1988**, *92*, 2874.
- (31) Diercksen, G. H. F.; Kraemer, W. P.; von Niessen, W. *Theor. Chim. Acta* **1972**, *28*, 67.
- (32) Yeo, G. A.; Ford, T. A. *Can. J. Chem.* **1991**, *69*, 632.

- (33) Ford, T. A. In *Molecular Interactions—From van der Waals to Strongly Bound Complexes*, Scheiner, S., Eds.; Wiley: New York, 1997.
- (34) Latajka, Z.; Scheiner, S. *J. Chem. Phys.* **1990**, *94*, 217.
- (35) Skurski, P.; Gutowski, M. *J. Chem. Phys.* **1998**, *108*, 6303.
- (36) Sadlej, J.; Moszynski, R.; Dobrowolski, J. Cz.; Mazurek, A. P. *J. Phys. Chem.* **1999**, *103*, 8528.
- (37) Tanabe, Y.; Rode, M. *J. Chem. Soc., Faraday Trans. 2* **1988**, *84*, 679.
- (38) Uras, N.; Buch, V.; Devlin, J. P. *J. Phys. Chem.* **2000**, *104*, 9203.
- (39) Sadlej, J.; Buch, V. *J. Chem. Phys.* **1994**, *100*, 4272.
- (40) Sandler, P.; oh Jung, J.; Szczesniak, M. M.; Buch, V. *J. Chem. Phys.* **1994**, *101*, 1378.
- (41) Sandler, P.; Buch, V.; Sadlej, J. *J. Chem. Phys.* **1996**, *105*, 10 387.
- (42) GAUSSIAN 94, Petersson, G. A.; Montgomery, J. A.; Raghavachari, K.; Al-Laham, M. A.; Zakrzewski, V. G.; Ortiz, J. V.; Foresman, J. B.; Cioslowski, J.; Stefanov, B. B.; Nanayakkara, A.; Challacombe, M.; Peng, C. Y.; Ayala, P. Y.; Chen, W.; Wong, M. W.; Andres, J. L.; Replogle, E. S.; Gomperts, R.; Martin, R. L.; Fox, D. J.; Binkley, J. S.; Defrees, D. J.; Baker, J.; Stewart, J. P.; Head-Gordon, M.; Gonzalez, C.; Pople, J. A. Gaussian, Inc., Pittsburgh, PA, 1995.
- (43) Boys, S. F.; Bernardi, F. *Mol. Phys.* **1970**, *19*, 553.
- (44) van Duijneveldt, F. B.; van Duijneveldt-van de Rijdt, J. G. C. M.; van Lenthe, J. H. *Chem. Rev.* **1994**, *94*, 1873.
- (45) Duijneveldt, F. B. In *Molecular Interactions – From van der Waals to Strongly Bound Complexes*, Scheiner, S., Eds.; Wiley: New York, 1997.
- (46) Turi, L.; Dannenberg, J. J. *J. Phys. Chem.* **1993**, *97*, 2488.
- (47) Hobza, P.; Bludsky, O.; Suhai, S. *Phys. Chem. Chem. Phys.* **1999**, *1*, 3073.
- (48) Dunning, T. H., Jr. *J. Chem. Phys.* **1989**, *90*, 1007.
- (49) Xantheas, S. S. *J. Chem. Phys.* **1994**, *100*, 7523.
- (50) Xantheas, S. S.; Dang, L. X. *J. Phys. Chem.* **1996**, *100*, 3989.
- (51) Xantheas, S. S.; Dunning, T. H. *J. Chem. Phys.* **1993**, *99*, 8774.
- (52) Rode, M. F.; Sadlej, J. *Chem. Phys. Lett.* **2001**, *342*, 220.
- (53) Milet, A.; Struniewicz, C.; Moszynski, R.; Sadlej, J.; Kisiel, Z.; Bialkowska-Jaworska, E.; Pszczolkowska, L. *Chem. Phys.* **2001**, *271*, 267.
- (54) Anderson, J. B. *J. Chem. Phys.* **1970**, *63*, 1499; Anderson, J. B. *J. Chem. Phys.* **1976**, *65*, 4121.
- (55) Shum, M. A.; Watts, R. O. *Phys. Rev.* **1991**, *204*, 293.
- (56) Buch, V. *J. Chem. Phys.* **1992**, *97*, 726.
- (57) Allen, M. P.; Tildesley, D. J. *Computer Simulation of Liquids*; Clarendon Press: Oxford, 1987.
- (58) Buch, V.; Sandler, P.; Sadlej, J. *J. Phys. Chem. B* **1998**, *102*, 8641.
- (59) Kuwajima, S.; Warshel, A. *J. Phys. Chem.* **1990**, *94*, 460.
- (60) Ahlstrom, P.; Wallqvist, A.; Engstrom, S.; Jonsson, B. *Mol. Phys.* **1989**, *68*, 563.
- (61) Szczesniak, M. M.; Rak, J.; Chalasinski, G. In *Recent Theoretical and Experimental Advances in Hydrogen Bonded Clusters*; Kluwer: Dordrecht, 2000.
- (62) Deng, Z.; Mortyna, G. J.; Klein, M. L. *J. Chem. Phys.* **1994**, *100*, 7590.